Journal of Solar Energy Engineering. Received October 14, 2022;
Accepted manuscript posted June 22, 2023. doi:10.1115/1.4063079

Compilation of a Solar Mirror Materials Database and an Analysis of Natural and Accelerated Mirror Exposure and Degradation

Tucker Farrell[1], Yue Cao[1], Frank Burkholder[2], Daniel Celvi[1], Christa Schreiber[1] and Guangdong Zhu[1*]
[1]National Renewable Energy Laboratory, 15013 Denver West Parkway, Golden CO, USA
[2]Replicant Consulting LLC.
[*]Corresponding Email: Guangdong.Zhu@nrel.gov

Abstract
The National Renewable Energy Laboratory (NREL) has been conducting exposure experiments on solar reflectors for over four decades. Thousands of mirror samples from over 100 suppliers have been exposed to and monitored in a range of relevant environments. These test conditions include outdoor test settings and several controlled laboratory environments. These samples have been rigorously individually characterized using a series of reflectance measurements, visual inspections, and in some cases, in-depth composition analysis to identify degradation modes, reflectance losses, and other mirror properties integral to understanding the solar reflector's life cycle. This paper compiles the decades of measurement data into a concise statistical analysis. It includes exposure and degradation data for numerous reflector types, including secondary-surface reflector permutations of polymer and glass superstrates with silver and aluminum reflectors as well as front-surface reflectors. The results herein are intended to analyze environmental stressors and degradation trends among various historical and state-of-the-art solar reflectors. This paper may be used to support solar reflector design, effective testing methodology, and inform manufacturing decisions moving forward. Presented are the results of the compiled database and an initial analysis for degradation rate modeling using full-spectrum and wavelength-dependent approaches. The database is a growing resource hosted on a live, publicly accessible website. In conjunction with the analysis presented here, the database provides a valuable resource to the solar reflector manufacturing and testing industry.

Nomenclature

Latin symbols

	b	Indicates a bounding parameter for exposure, in months
	k	Tolerance coefficient
	t	Duration of exposure, in months unless otherwise specified

Greek symbols

	β	Degradation rate in % Reflectance loss/month
	λ	Wavelength in nanometers
	$\Delta\rho$	Reflectance loss, in % reflectivity

Subscripts

	ac	Accelerated condition
	l	Lower bound, in exposure months
	od	Outdoor condition
	u	Upper bound, in exposure months

Abbreviations

	AF	Acceleration factor

Journal of Solar Energy Engineering. Received October 14, 2022;
Accepted manuscript posted June 22, 2023. doi:10.1115/1.4063079

DNI	Direct-normal irradiance
SWV	Solar-weighted Value
VBR	Variation-band-ratio
XALE	Xenon Arc Lamp Exposure

1 Introduction

Solar reflectors for concentrating solar power are exposed to harsh operational conditions for the duration of their operational life [1,2]. With the mirrors alone representing anywhere from 10% to 50% [2] of the plant installation cost, modeling their durability and optical performance is integral to maintaining a financially viable energy source [3]. Reflectors must be designed to maintain high reflectance, aiming for 95% reflectivity and a lifespan of 15–30 years [1,4–6], to ensure the highest percentage of incident energy is reflected onto the receiver. Degradation to specular reflectance can be especially problematic, where losses in reflectance and poor monitoring can result in financial losses in the tens of millions of US dollars, and up to 40% of performance. [7–9]

Research has largely established the importance of monitoring reflectance properties through soiling studies [10–12], exposure experiments [13–15], proposed modeling techniques [1,16], and proposed standardization [13,17]. These exposure experiments may be limited to mere months of exposure. The outdoor natural degradation periods can be several decades; far too long to run practical experiment [3]. At a minimum, the techniques cited here will benefit from the publication of additional degradation and long-term exposure data. The data presented herein dates to 1980 with exposure experiments lasting decades, well into the design life of a reflector. Initial outdoor exposure results are available in 2020 conference proceedings. [18]

A gap in knowledge exists around the degradation rate and fundamental mechanisms for solar reflectors. Among the most recent standardization experiments, the Spanish Association for Standardization and Certification (AENOR) durability verification round-robin [13] presented acceptable agreement between five research laboratories, but resulted in high uncertainty and tested only three samples per condition. Accelerated aging tests and modeling techniques have not been comprehensively researched and validated to accurately predict the performance of the wide range of solar mirrors over their projected life cycle. The establishment and initial analysis on NREL's Solar Mirror Materials Database (SMMD) is a crucial step toward creating a centralized, reliable, and established method for solar mirror accelerated aging procedures, modeling, and life cycle performance analysis supported by a large volume of statistically significant data.

2 Equipment and instruments for mirror degradation tests

At NREL, mirror samples are typically exposed either in indoor/outdoor equipment with accelerated conditions or at natural test sites at various locations. At each given time (before, during, and after each degradation test), mirror samples can be characterized with reflectance measurement and coating material.

Equipment used for accelerated aging tests is summarized in Table 1. Instruments measuring solar reflectance are given in Table 2. A reflectance characterization for a solar reflector will optimally collect data on solar weighted values (SWV) calculated from a full spectral measurement from 250–2,500 nm following ASTM Standard for solar spectral irradiances [19] and a specularity derivation [8], which may be monochromatic or collected at several wavelengths in accordance with the SolarPACES guideline for

Journal of Solar Energy Engineering. Received October 14, 2022;
Accepted manuscript posted June 22, 2023. doi:10.1115/1.4063079

measurement [20]. To fully characterize the reflection, the recommendation is a laboratory spectrophotometer with near-normal incidence, an integrating sphere, and wavelength resolution of 5 nm or better. NREL uses the PerkinElmer Lambda 1050. This can be used in conjunction with a specular reflectometer such as the Devices and Services 15R-USB, which measures monochromatic reflectance at varying acceptance apertures at a fixed incidence angle. The SOC is sufficient in field measurements, supplemental lab measurements, and useful for surface uniformity metrics. In addition, various material characterization technologies shown in Table 12 may be employed to better understand the degradation mechanism of coating layers on mirrors under different exposure conditions.

Table 1: Summary of equipment for accelerated aging tests.

Equipment	Test Parameters
XALE: Xenon Arc Lamp Exposure (Atlas Ci5000)	Heat, Humidity, UV Irradiance, Water Spray
EMMAQUA: Equatorial Mount with Mirrors for Acceleration with Water (aqua)	Heat, Water Spray, Solar Spectrum Irradiance
UAWS: Ultra Accelerated Weathering System	Heat, UV Irradiance
CASS: Copper Accelerated Salt Spray	Heat, Salt Spray (Deposition), Humidity
NSS: Neutral Salt Spray	Heat, Salt Spray (Deposition), Humidity
Suntest XXL+ (Xe) & Sepap 12/24 (Hg) from ATLAS MTS and UV5X (HMI) from AMC/AMTC/BIA	Heat, Humidity, UV Irradiance, Water Spray

Table 2: Summary of the instruments and settings used for measurements.

Instrument	Measurement Type	Wavelength Ranges	Incidence Angle	Measured Spot Size	Measurements per sample
L1050/950	Hemispherical	250–2,500 nm, 5-nm increments	8°	0.50 cm^2	3
Devices and Services 15R -USB (D&S)	Specular (15 mrad, 25 mrad, 46 mrad)	660-nm peak irradiance	15°	$(5.1*10^{-4})$ cm^2	5
Surface Optics Corporation (SOC) Solar 410	Hemispherical /Specular	Bands from 335–2,500 nm	Near normal	0.18 cm^2	20

3 Solar Mirror Materials Database (SMMD)

3.1 Database contents

Over the past four decades, NREL's optical material characterization lab has conducted solar mirror degradation tests and documented reflectance degradation under various test conditions, which includes accelerated aging conditions and natural outdoor conditions at various locations. A solar mirror materials database (SMMD) has been compiled in a digital format to facilitate data analysis. Table 3 summarizes statistical attributes of the newly established SMMD, where a mirror "variant" is defined as a specific manufacturer and mirror construction, i.e. front-surface aluminum, glass-silver, polymer-silver, etc. In this case, manufacturer A, glass-silver will be a different "variant" than manufacturer B glass-silver.

Journal of Solar Energy Engineering. Received October 14, 2022;
Accepted manuscript posted June 22, 2023. doi:10.1115/1.4063079

Table 3: Statistical attributes of the newly developed SMMD. "Valid" measurements are the number of measurements remaining after the screening process presented in Section 4.2

Database properties	**Value**	**Notes:**
Initial Test Year	1980	
Number of Mirror Manufacturers	116	
Number of Mirror Variants	197	One mirror manufacturer often provides more than one type of mirror.
Number of Mirror Samples	2,414	There are typically several samples provided for a given mirror type.
Test Conditions	XALE: - Temperature: 60°C - Humidity: 60% - Full-spectrum solar irradiation: 2,125 W/m^2 (0.7 W/m^2/nm at 340 nm)	A group of samples may be distributed across various test conditions. An acceleration factor will be calculated by comparing degradation rates measured at the XALE condition and one outdoor condition.
	Golden, CO	
	Phoenix, AZ	
	Miami, FL	
Test Duration (Months)	0.89–108.31 (XALE)	
	1.58–154.74 (Golden, CO)	
	0.01–121.01 (Phoenix, AZ)	
	0.01–113.24 (Miami, FL)	
Number of L1050 Measurements	68,611 (24,036 valid)	One L1050 scan measures one specific mirror sample at a given exposure time at a given test condition. Nominally 3 scans are taken, rotating the sample 90° between each measurement.
Number of D&S Measurements	62,250 (62,250 valid)	One D&S measures 3 to 5 spots over one specific mirror sample at a given exposure time at a given test condition; in most of cases, 25 mrad aperture is used for the D&S reflectometer.
Number of Experiments	383	One experiment is defined as a set of samples undergoing a test condition for a given test period. Sample size varies from experiment to experiment.

3.2 Test conditions

All mirror samples in the SMMD were tested with at least one of four test conditions:
1. Indoors under accelerated XALE conditions
2. Outdoors in Miami, FL
3. Outdoors in Phoenix, AZ
4. Outdoors in Golden, CO

These samples are tested under variable experimental conditions. Measurement frequency may vary between experiments and sites. The environmental parameters for the listed test conditions are

Journal of Solar Energy Engineering. Received October 14, 2022;
Accepted manuscript posted June 22, 2023. doi:10.1115/1.4063079

summarized in Table 4. Temperature differences are defined as average and maximum daily temperature swings experienced in each environment. The XALE conditions expose the samples to the harshest weathering conditions with respect to solar irradiation intensity measured in direct normal irradiance (DNI) and isothermal temperature. Among the three outdoor conditions, the test station in Phoenix, AZ has the lowest humidity, highest daily temperature, and largest temperature difference over a year; the test station in Miami, FL has the highest humidity and a relatively stable temperature over a year; and the station in Golden, CO has the lowest average temperature but large temperature differences over a year.

Table 4: Testing condition attributes for different locations

Location	Annual DNI (MWh/m^2)*	Average Relative Humidity (%)	Average Temperature (ºC)	Max Temperature (ºC)	Average Temperature Difference (ºC)	Max Temperature Difference (ºC)
Phoenix, AZ	2.68	34.99	22.25	48	15.18	22
Miami, FL	1.99	80.04	24.58	30	2.72	9
Golden, CO	1.98	56.22	8.76	36	13.24	22
XALE	18.61	60	60	60	0	0

*Total annual DNI for three outdoor locations were obtained by averaging the DNI over many years when weather data are available.

4 Solar mirror degradation analysis

This section provides an initial analysis of solar mirror degradation. The samples exposed in the listed test conditions can be analyzed for changes and losses in reflectance, then correlated with the environmental conditions in which they were weathered. Several reflector types were weathered in various test conditions, creating an opportunity for comparison and correlation of environmental stressors to reflectance degradation.

First, we screen the data for strong correlations and calculate a degradation rate on suitable samples. In this analysis, a degradation rate is the linearly approximated reflectance loss over time. We choose linear due to the wide range of data and simplicity of the model. Specific studies analyzing the beginning or end-of-life degradation trends may be better suited by a separate statistical analysis. Strongly correlated degradation rates can be used for comparisons among similar sample types to gain insights into critical environmental parameters.

Second, we can leverage these insights to estimate acceleration factors, or appropriate abbreviated weathering times in harsher, controlled environmental conditions to model longer outdoor exposure effects. These accelerated weathering conditions, when appropriately supported by the data, can be used to test weathering effects on new solar reflectors using the most relevant environmental inputs.

Finally, we look at the wavelength-dependent degradation for suitable mirror types. Degradation manifesting as impacts to a reflector's SWV does not guarantee the reflector is degrading uniformly across the input spectrum. Compositional changes such as solarization of reflector glass may cause wavelength-dependent impacts to reflectance that are not captured by SWV alone.

4.1 Calculating a degradation rate for a solar mirror

Journal of Solar Energy Engineering. Received October 14, 2022;
Accepted manuscript posted June 22, 2023. doi:10.1115/1.4063079

The reflectance of a mirror sample will degrade over time when exposed to a given test condition. Assuming a constant degradation rate, the change in reflectance of a given mirror sample can be modeled in Equation (1):

$$\Delta\rho(t) = \beta t \quad (1)$$

where:
$\Delta\rho$ is the reflectance difference between the original reflectance and the degraded reflectance after a prescribed exposure period.
β is the degradation rate (%R per month).
t is the months of exposure at a given test condition

The acceleration factor *AF* for a given accelerated test condition *ac* and a reference outdoor condition *od* is then calculated in Equation (2):

$$\mathrm{AF} = \frac{\beta_{ac}}{\beta_{od}}. \quad (2)$$

Degradation rate may be calculated using a solar-weighted hemispherical reflectance, a monochromatic reflectance (D&S), or be analyzed as a function of wavelength, as seen in Section 4.4.

4.2 Screening the database for suitable samples

The database contains over 2,000 samples and over 100,000 measurements over 197 distinct mirror types; see Table 3. To perform meaningful degradation analyses, data are screened in three primary steps for suitable samples.

a. Consider only valid measurements.

Included measurements may be witness scans, calibration scans, erroneous measurements due to operator error, equipment malfunction, or otherwise. Unsuitable data are filtered out and discarded by seeking out and discarding measurements that do not:

- Have an established sample ID with associated material properties.
- Have a logged exposure condition.
- Have a reflectance value between 0 and 100%

This yields 383 experiments with reflectance data that is not misidentified or an obvious misrepresentation.

b. Multiple exposure conditions

To perform the degradation rate calculation, the analysis requires a minimum of two exposure conditions. One of these must be indoor, XALE condition. Any number of remaining conditions will be outdoor conditions with available climate data. The SMMD contains sample data for four primary weather conditions, summarized in Table 5. The samples with multiple exposure conditions are advanced to the next screening criterium.

Journal of Solar Energy Engineering. Received October 14, 2022;
Accepted manuscript posted June 22, 2023. doi:10.1115/1.4063079

c. Correlation analysis using R^2

A thorough R^2 analysis is conducted over the valid samples from steps a and b above to identify samples with identifiable degradation trends. Degradation rate may be based on L1050 or D&S measurements. Figure 1 gives R^2 correlation statistics of linear degradation regression fitting for both L1050 SWVs and D&S reflectance values. As shown, about 15% of test experiments using the L1050 SWV and 40% of experiments using the D&S measurements give rise to $R^2 > 0.7$. This suggests D&S measurements may give more reliable degradation characterizations than the L1050. The possible reason may be because: (1) D&S measures five spots on a mirror sample, in comparison to three spots by L1050; or (2) D&S measurement surface area is much smaller than that by L1050, which may be less impacted by mirror surface variation.

R^2 distribution statistics are further analyzed for correlations between instruments and varying exposure conditions, shown in Figure 2. In general, measurements by both L1050 and D&S show stronger correlation in the XALE test environment than in outdoor tests.

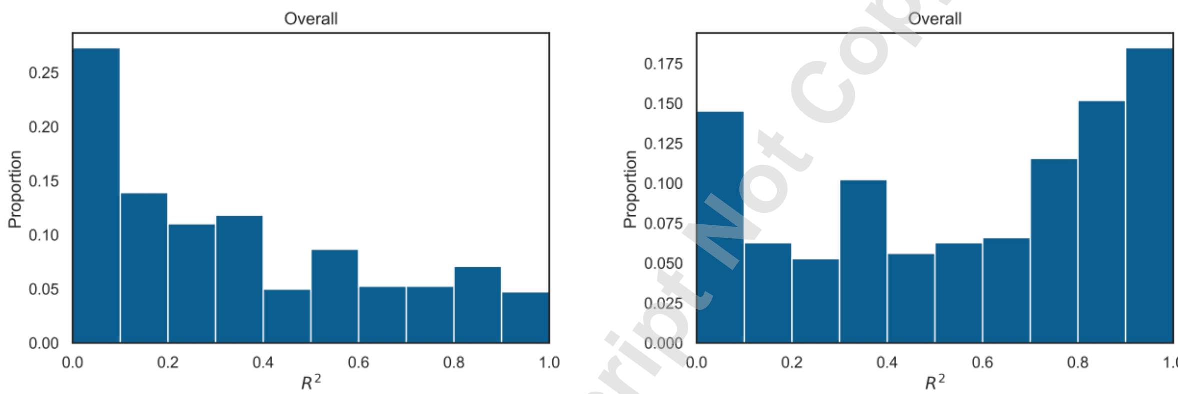

(a) L1050 SWV R^2 distribution. (b) D&S R^2 distribution.

Figure 1: Statistics of R^2 over entire database (L1050 and D&S).

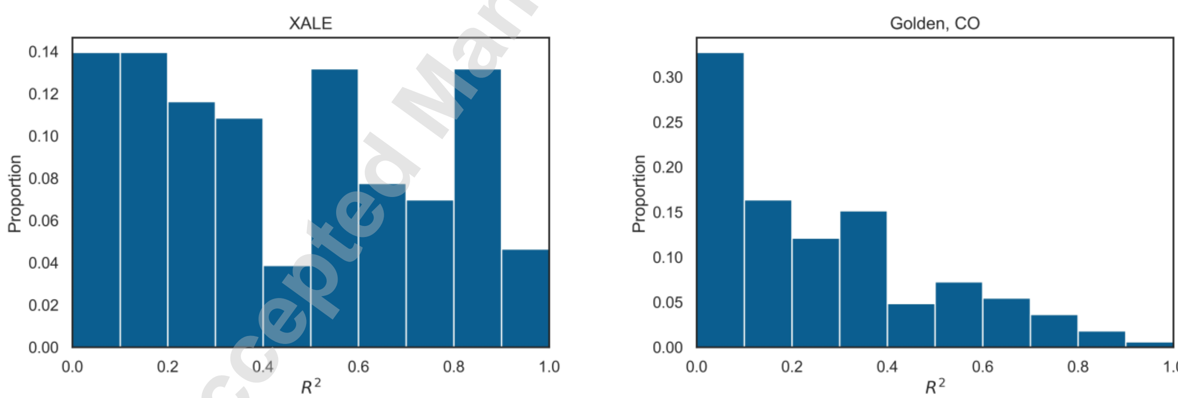

(a) L1050 SWV in XALE (b) L1050 SWV in Golden, CO

Journal of Solar Energy Engineering. Received October 14, 2022;
Accepted manuscript posted June 22, 2023. doi:10.1115/1.4063079

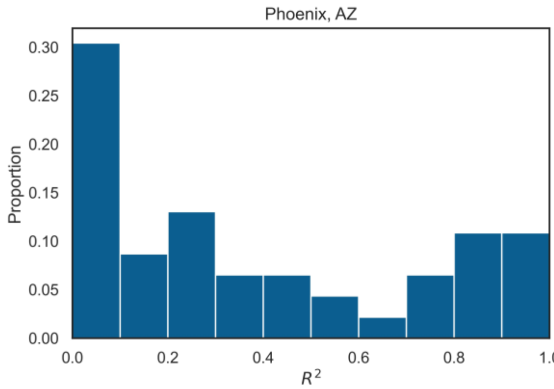

(c) L1050 SWV in Phoenix, AZ

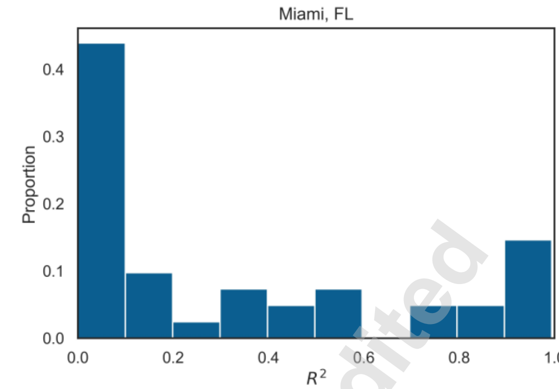

(d) L1050 SWV in Miami, FL

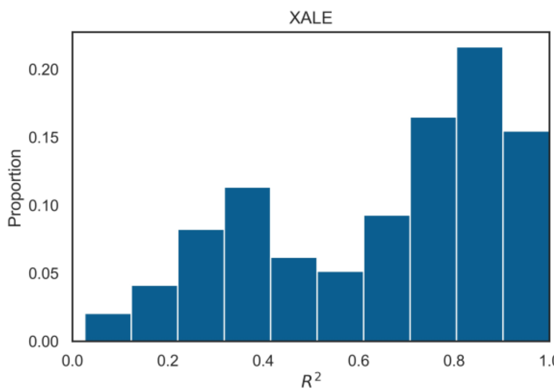

(e) D&S in XALE

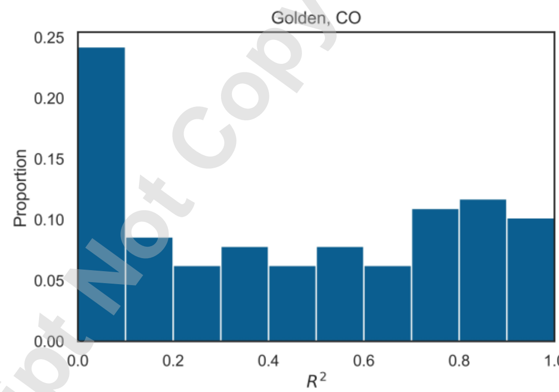

(f) D&S in Golden, CO

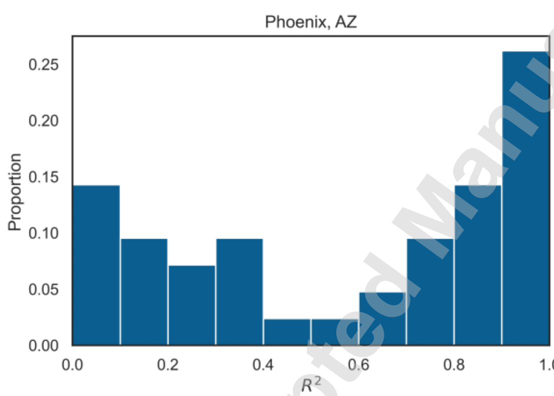

(g) D&S in Phoenix, AZ

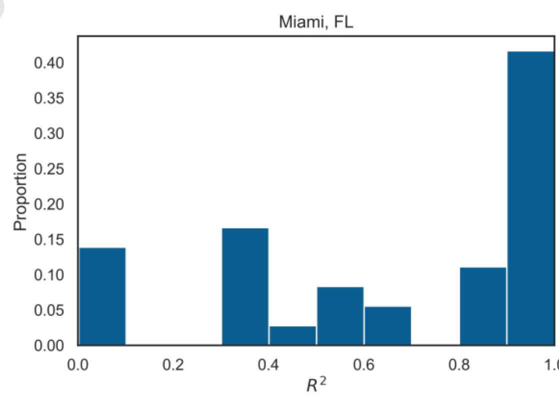

(h) D&S in Miami, FL

Figure 2: Statistics of R^2 over entire database broken into individual test condition and measurement method.

Degradation experiments with $R^2 > 0.75$ are first selected for analysis. Each experiment uses the same batch/type of mirror samples split into multiple sets. Each set is tested under a given test condition. Table 5 summarizes all experiments with a specific type of mirror sample with all test conditions, in which the R^2 of linear regression fitting over the data points is greater than 0.75.

Journal of Solar Energy Engineering. Received October 14, 2022;
Accepted manuscript posted June 22, 2023. doi:10.1115/1.4063079

Table 5: Mirror samples meeting the requirements: $R^2 > 0.75$ and two or more test conditions.

	Mirror manufacturer and sample ID	Test Conditions	Mirror Formation
1	JDSU-1	L1050: XALE, Miami, FL D&S: XALE, Golden, CO, Phoenix, AZ, Miami, FL	Glass-Aluminum
2	ReflecTech-5	L1050: XALE, Golden, CO, Phoenix, AZ, Miami, FL D&S: XALE, Miami, FL	Polymer-Silver
3	Alanod-7	D&S: XALE, Golden, CO, Phoenix, AZ, Miami, FL	Polymer-Aluminum
4	Valspar-1	D&S: XALE, Phoenix, AZ, Miami, FL	Glass-Silver
5	Aluminum-9	L1050: Golden, CO, Miami, FL D&S: Phoenix, AZ, Miami, FL	Polymer-Aluminum
6	Naugatuck-9	L1050: XALE, Golden, CO	Glass-Silver
7	Alcoa-8a	D&S: XALE, Golden, CO	Polymer-Aluminum
8	Samsung-2	D&S: XALE, Phoenix, AZ	Glass-Silver
9	AirlightEnergy-1	L1050: XALE, Miami, FL D&S: Phoenix, AZ, Miami, FL	Polymer-Aluminum
10	Alcoa-11	L1050: Phoenix, AZ, Miami, FL D&S: XALE, Phoenix, AZ	Polymer-Aluminum
11	Samsung-3	D&S: XALE, Miami, FL	Glass-Silver
12	Guardian-1	L1050: Phoenix, AZ, Miami, FL	Glass-Silver
13	Alanod-8	L1050: Phoenix, AZ, Miami, FL D&S: Phoenix, AZ, Miami, FL	Polymer-Aluminum
14	DunMore-3	L1050: Phoenix, AZ, Miami, FL D&S: Phoenix, AZ, Miami, FL	Aluminum-Aluminum
15	PPG-4	D&S: Phoenix, AZ, Miami, FL	Glass-Silver
16	Fenzi-1	L1050: XALE, Golden, CO D&S: XALE, Miami, FL	Glass-Silver
17	Alcoa-9	D&S: XALE, Golden, CO	Unknown
18	AGC-1	D&S: XALE, Miami, FL	Glass-Silver
19	Alanod-6b	D&S: XALE, Golden, CO	Polymer-Aluminum
20	Naugatuck-15	D&S: XALE, Golden, CO	Glass-Silver
21	SAIC_McLean-6	D&S: XALE, Golden, CO	Unknown
22	3M-4	D&S: Phoenix, AZ, Miami, FL	Polymer-Silver
23	Alanod-2b	D&S: Phoenix, AZ, Miami, FL	Polymer-Aluminum
24	Alanod-4	D&S: Golden, CO, Miami, FL	Polymer-Aluminum
25	ECP-7	D&S: Golden, CO, Phoenix, AZ	Polymer-Silver
26	IEA-3	D&S: Phoenix, AZ, Miami, FL	Unknown
27	SA85-3	D&S: Golden, CO, Phoenix, AZ	Polymer-Aluminum
28	Abengoa-5	D&S: XALE, Golden, CO	Polymer-Silver
29	ECP-2	D&S: Golden, CO, Miami, FL	Polymer-Silver
30	ReflecTech-3	D&S: XALE, Golden, CO	Polymer-Silver
31	Abengoa-4	D&S: XALE, Golden, CO	Unknown

Figure 4 gives degradation rates at selected example test conditions for all experiments with R^2 greater than 0.75.

4.3 Degradation rate analysis on SMMD suitable data

Journal of Solar Energy Engineering. Received October 14, 2022;
Accepted manuscript posted June 22, 2023. doi:10.1115/1.4063079

Once the database is screened for suitable samples, a degradation rate analysis is done on the selected experiments. Here, β_{ac} is the degradation rate when exposed to the accelerated test condition, and β_{od} is degradation rate of the reference outdoor condition.

In the compiled SMMD, a given experiment may include multiple samples tested under a given test condition and exposure duration. During the test period, the mirror samples may be measured multiple times. Figure 3 gives a few examples of SWV reflectance as a function of exposure time in months. SWV is based on the reflectance measurements by L1050 across the 250–2,500 nm spectral range, and calculated according to the spectral weights presented in ASTM G173D [19]. Degradation rate based on SWV can then be calculated by using the slope of a fitting line on all the data points. The coefficient of determination, R^2, can be used to indicate the variance of data points from the predicted linear regression. Each plot in the figure corresponds to data points in an experiment, which may include more than one mirror sample as shown. Four examples give rise to a wide range of R^2, from 0.0001 to 0.838. A low R^2 indicates an inability of a linear regression to model the data points, thus lower confidence on the calculation of the degradation rate. For example, Figure 4 (a) may indicate discrepancies in data collection, or measurement techniques. The data here would not be suitable for degradation analysis. Figure 4 (d) however, shows a strong linear correlation over the exposure period.

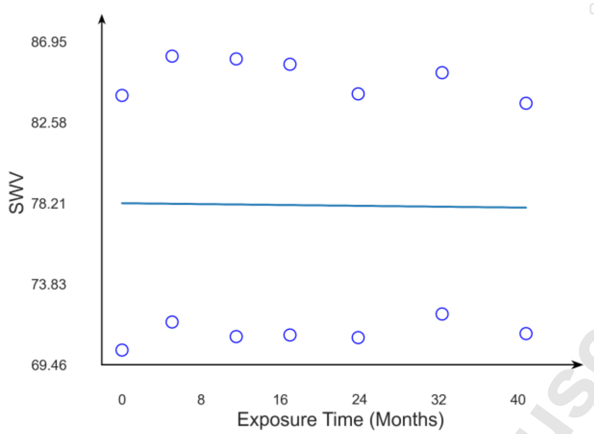

(a) Winston-1 mirror with $R^2 = 0.0001$

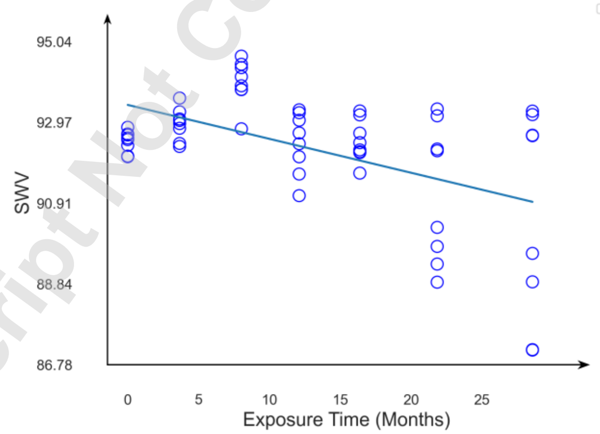

(b) Alcoa-8a mirror with $R^2 = 0.258$

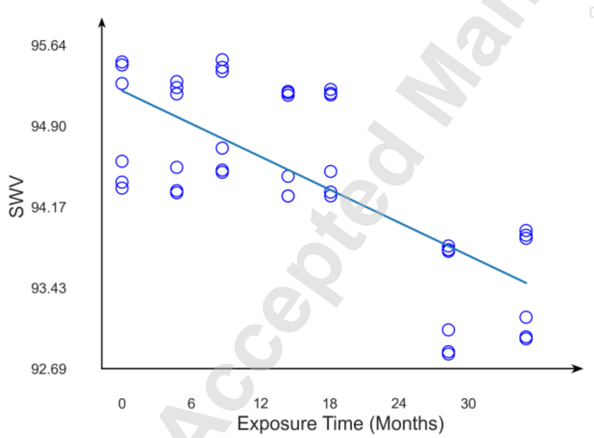

(c) SaintGobain-2 mirror with $R^2 = 0.533$

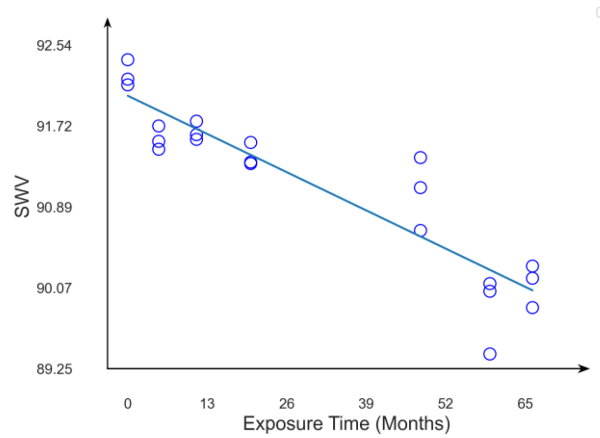

(d) Naugatuck-9 mirror with $R^2 = 0.838$

Figure 3: Degradation rate of various mirror test experiments by using linear regression fitting with corresponding R^2.

Journal of Solar Energy Engineering. Received October 14, 2022;
Accepted manuscript posted June 22, 2023. doi:10.1115/1.4063079

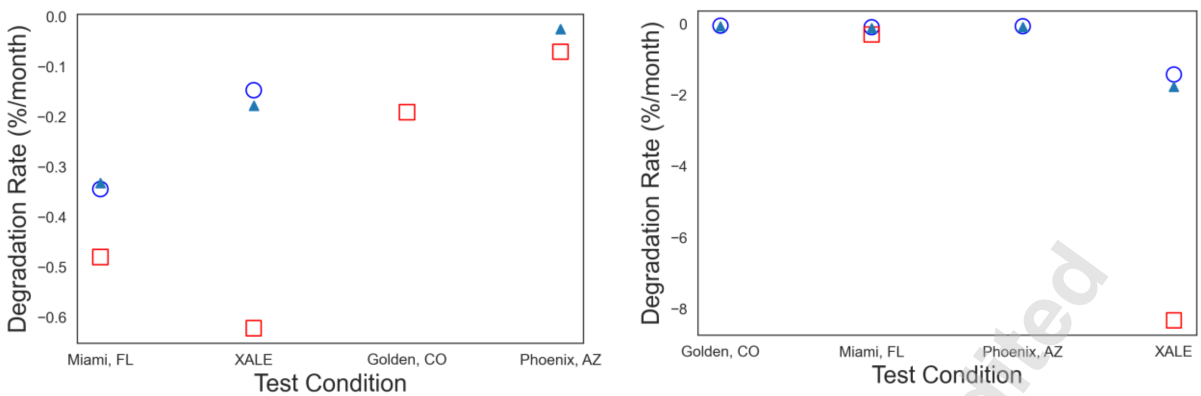

(a) JDSU-1 (b) ReflecTech-5

Figure 4: Example degradation rates for two experiments with R2 > 0.75 at difference test conditions. Circular points show L1050 measurements. Square points represent D&S measurements. Triangular points are the degradation rates at 660 nm computed from L1050 data.

A given test condition can be characterized with various parameters, such as average temperature, DNI, or temperature variation during a given duration (a day or year). Various test conditions have their own parameters. Typically, XALE stands as the harshest exposure condition with the highest temperature and solar irradiation intensity. Table 4 illustrates a comparison of weather attributes for various test conditions.

Secondly, we group experiments that are tested under the same conditions (e.g., Naugatuck-9 and Fenzi-1 from an L1050 experiment that tested both in Golden, CO and XALE). Within these subgroups, degradation rates between the outdoor and XALE exposure conditions can be compared, with the higher degradation rates implying more influential weather conditions. For example, in the case of the Naugatuck-9 and Fenzi-1 mirrors, both degradation rates under XALE conditions are higher. XALE has larger DNI, higher average temperature, and higher maximum temperature than Golden, CO. Then we check those three indices as impacts on degradation rate. We apply that metric to experiments and summarize the results in Table 6 for L1050 measurements and Table 7 for D&S measurements.

Table 6: L1050 relation between degradation rates and weather conditions. The check mark signifies that in a comparison between exposure conditions, the higher degradation rate resulted from more extreme exposure conditions in the marked category.

Experiment	**Material**	**DNI**	**Relative Humidity**	**Average Temperature**	**Max Temperature**	**Average Temperature Difference**	**Max Temperature Difference**
ReflecTech-5	Polymer-Silver	✓		✓	✓		
Naugatuck-9	Glass-Silver	✓		✓	✓		
Fenzi-1	Glass-Silver	✓		✓	✓		
Aluminum-9	Polymer-Aluminum		✓	✓			
Guardian-1	Glass-Silver	✓			✓	✓	✓
DunMore-3	Aluminum-Aluminum		✓				
JDSU-1	Glass-Aluminum		✓			✓	✓
Total count		4	3	4	4	2	2

Journal of Solar Energy Engineering. Received October 14, 2022;
Accepted manuscript posted June 22, 2023. doi:10.1115/1.4063079

A higher tally in a column indicates that the parameter is more influential when compared to all parameters examined. For example, in L1050 experiments, the most influential stressors are DNI, maximum temperature, and average temperature. Relative humidity is also influential. Average temperature difference and max temperature difference are less influential. The same methodology is followed for the D&S experiments.

Table 7: D&S relation between degradation rates and weather conditions.

Experiment	Material	DNI	Relative Humidity	Average Temperature	Max Temperature	Average Temperature Difference	Max Temperature Difference
Alanod-7	Polymer-Aluminum	✓		✓	✓		
JDSU-1	Glass-Aluminum	✓	✓	✓	✓		
Valspar-1	Glass-Silver	✓	✓	✓	✓		
ECP-7	Polymer-Silver	✓		✓	✓	✓	
SA85-3	Polymer-Aluminum	✓		✓	✓	✓	
Alanod-6b	Polymer-Aluminum	✓		✓	✓		
Naugatuck-15	Glass-Silver	✓		✓	✓		
SAIC_McLean -6	Unknown					✓	✓
ReflecTech-3	Polymer-Silver	✓		✓	✓		
Alanod-4	Polymer-Aluminum		✓	✓			
Samsung-2	Glass-Silver	✓	✓	✓	✓		
PPG-4	Glass-Silver		✓				
3M-4	Polymer-Silver		✓				
Alanod-2b	Polymer-Aluminum		✓				
Aluminum-9	Polymer-Aluminum		✓				
IEA-3	Unknown		✓				
Fenzi-1	Glass-Silver	✓	✓	✓	✓		
AGC-1	Glass-Silver	✓	✓	✓	✓		
Samsung-3	Glass-Silver	✓	✓	✓	✓		
Total		12	12	13	12	3	1

For D&S experiments, average temperature is the most influential, followed by DNI, relative humidity and maximum temperature. Average and maximum temperature differences are not influential.

4.4 Wavelength-dependent degradation rate between XALE and outdoor conditions

4.4.1 Formulation

Journal of Solar Energy Engineering. Received October 14, 2022;
Accepted manuscript posted June 22, 2023. doi:10.1115/1.4063079

In this section, we analyze the relationship between wavelength and degradation rate. Based on degradation rate with respect to wavelength plots in Figure 5, we propose a relationship in Equation (3) based on the proposed in Section 4.1, modified to depend on wavelength:

$$\beta_\lambda = \frac{p}{\lambda} + \mathrm{b} \tag{3}$$

Here, β_λ is the degradation rate at a specific wavelength, and λ is the wavelength. We apply wavelengths from 250 nm to 2,500 nm with 50-nm increment. A linear regression model is applied to compute p and b, to continuously model degradation rates across the discrete datapoints. The acceleration factor (AF) is the ratio of degradation rates between XALE and other test conditions at each wavelength.
Data were filtered according to the following rules:

a. There are two more test conditions including XALE
b. R^2 in previous section is greater than 0.75, or 0.5
c. Degradation rate is < 0 (mirror reflectance did not increase)

4.4.2 Numerical test

In Figure 5 (a), points and corresponding fitted lines indicate data points and associated regression curves. XALE is shown in red, Golden, CO in purple, Phoenix, AZ in blue and Miami, FL in green. In Figure 5 (b), points indicate fitted values from proposed formula. The solid line means average value of fitted values. The dashed line means two standard deviation value plus or minus average value.

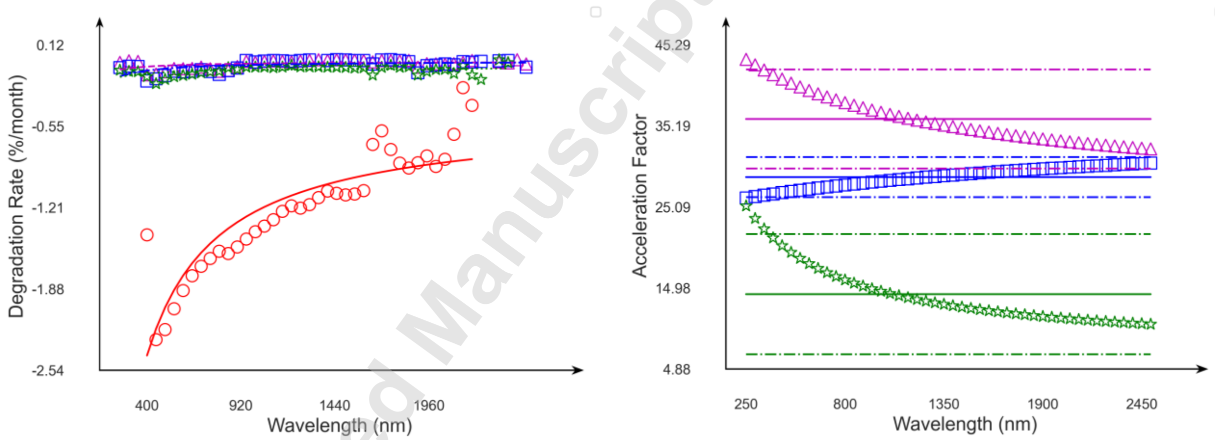

(a) ReflecTech-5 degradation rate and fitted line

(b) ReflecTech-5 acceleration factors

Figure 5: Example fitted curves and acceleration factors for an experiment with $R^2 > 0.75$. (a) The spectral responses with appropriate fitted curves delineated by weather condition. (b) The wavelength-dependent acceleration factors when compared with the XALE condition. 2σ bounds are shown in dashed lines, indicating the variation in acceleration factors across the measured spectrum. Colors follow the same delineation as in (a).

Journal of Solar Energy Engineering. Received October 14, 2022;
Accepted manuscript posted June 22, 2023. doi:10.1115/1.4063079

Table 8: Wavelength and degradation rate analysis. p and b are coefficients of the formula. R^2 is from the linear regression. Here we use $R^2 > 0.75$.

Mirror Type	Test Condition	p	b	R2	Degradation Rate		Acceleration Factor	
					Mean	Std. Dev.	Mean	Std. Dev.
Naugatuck-9	Golden, CO	14.14	0.00	0.29	-0.02	0.02	3.96	4.23
Naugatuck-9	XALE	211.79	0.11	0.91	-0.12	0.18	NAN	NAN
JDSU-1	Miami, FL	0.44	-0.39	0.00	-0.39	0.16	0.33	0.19
JDSU-1	XALE	92.68	-0.03	0.60	-0.13	0.10	NAN	NAN
Fenzi-1	XALE	107.30	0.03	0.42	-0.09	0.13	NAN	NAN
Fenzi-1	Golden, CO	75.83	0.00	0.47	-0.07	0.08	0.98	0.22
ReflecTech-5	Golden, CO	16.36	-0.02	0.16	-0.04	0.03	36.02	3.09
ReflecTech-5	Phoenix, AZ	31.15	-0.01	0.31	-0.05	0.05	28.79	1.25
ReflecTech-5	Miami, FL	19.17	-0.07	0.16	-0.09	0.04	14.20	3.74
ReflecTech-5	XALE	785.28	-0.46	0.74	-1.21	0.48	NAN	NAN
AirlightEnergy-1	Miami, FL	476.81	-1.29	0.36	-1.74	0.47	1.92	0.21
AirlightEnergy-1	XALE	1535.94	-1.91	0.28	-3.46	1.57	NAN	NAN

Table 9 summarizes the wavelength-dependent acceleration factors or all samples with a correlation coefficient $R^2 > 0.75$. If we include all samples with R^2 in (0.5, 0.75], an additional 13 samples are analyzed. Results of this analysis are shown in Table 10. Note that in Tables 9 and 10, the reported correlation statistic in the R2 column is different than the correlation metric used to filter the experiment. The former is computed from the wavelength-dependent data, while the latter is the SWV degradation rate computed as in Section 4.3.

Table 9: Wavelength and degradation rate analysis. p and b are coefficient of formula. R^2 is from linear regression. Here we use R^2 is in (0.5, 0.75].

Mirror variant	Test condition	p	b	R2	Degradation rate		Acceleration factor	
					Mean	Std. Dev.	Mean	Std. Dev.
3M_Northbridge-6	Golden, CO	562.71	0.58	0.71	-0.29	0.30	9.18	33.70
3M_Northbridge-6	XALE	5973.41	4.34	0.86	-2.61	3.36	NAN	NAN
3M-9	Golden, CO	88.66	-0.07	0.14	-0.17	0.20	1.86	0.28
3M-9	XALE	249.47	-0.06	0.16	-0.35	0.51	NAN	NAN
Alcoa-11	Golden, CO	-14.41	-0.07	0.12	-0.06	0.03	2.36	3.41
Alcoa-11	Phoenix, AZ	66.48	-0.03	0.61	-0.09	0.06	0.99	0.07
Alcoa-11	Miami, FL	31.77	-0.10	0.23	-0.13	0.05	0.69	0.15
Alcoa-11	XALE	52.93	-0.04	0.45	-0.09	0.05	NAN	NAN
Alcoa-12	Golden, CO	-7.94	-0.05	0.12	-0.04	0.01	2.12	1.09
Alcoa-12	XALE	17.22	-0.06	0.07	-0.08	0.04	NAN	NAN
CoolEarth-1	Miami, FL	793.29	-0.79	0.97	-1.62	0.65	3.64	0.84
CoolEarth-1	XALE	376.14	-5.02	0.39	-5.42	0.49	NAN	NAN
DunMore-1	Golden, CO	89.48	0.01	0.84	-0.09	0.08	3.80	1.36
DunMore-1	XALE	104.71	-0.15	0.71	-0.26	0.10	NAN	NAN
Flabeg-3	Golden, CO	24.91	0.00	0.32	-0.03	0.04	3.18	0.10
Flabeg-3	Phoenix, AZ	42.85	-0.01	0.30	-0.07	0.08	1.52	0.09
Flabeg-3	XALE	74.18	0.00	0.41	-0.08	0.09	NAN	NAN
Naugatuck-17	Golden, CO	8.55	-0.03	0.05	-0.05	0.04	8.24	0.65
Naugatuck-17	XALE	111.55	-0.22	0.20	-0.34	0.20	NAN	NAN
SaintGobain-1a	XALE	44.41	-0.02	0.41	-0.07	0.06	NAN	NAN
SaintGobain-1a	Phoenix, AZ	38.94	-0.01	0.24	-0.08	0.08	1.34	0.08
Samsung-2	Phoenix, AZ	45.15	-0.01	0.26	-0.08	0.09	3.62	0.93
Samsung-2	XALE	276.90	0.04	0.39	-0.26	0.36	NAN	NAN

Journal of Solar Energy Engineering. Received October 14, 2022;
Accepted manuscript posted June 22, 2023. doi:10.1115/1.4063079

SolarSystems-20	Golden, CO	17.39	-0.01	0.41	-0.02	0.02	34.94	2.83
SolarSystems-20	XALE	477.67	-0.28	0.86	-0.78	0.41	NAN	NAN
SolarSystems-23	Golden, CO	37.11	0.00	0.50	-0.04	0.04	8.99	3.30
SolarSystems-23	XALE	83.66	-0.18	0.21	-0.26	0.15	NAN	NAN
Valspar-1	Phoenix, AZ	347.15	0.11	0.60	-0.22	0.27	0.46	0.09
Valspar-1	XALE	124.30	0.03	0.54	-0.10	0.13	NAN	NAN

4.4.3 Variation-band-ratio

We propose an index, variation-band ratio (VBR), which is the ratio of 2σ, or twice the standard deviation, and the mean value μ of the acceleration factors across all wavelengths. All experiments listed in Table 9 are computed. A low VBR indicates a sample that degrades consistently across each wavelength. A high VBR implies degradation rate varies substantially with wavelength. For example, glass-silver mirrors in Figure 6 (c) show lower VBRs than that of aluminum in Figure 6 (b) or polymer-coated mirrors in Figure 6 (d) and Figure 6 (e). This indicates glass-covered mirrors may degrade more consistently across the solar spectrum.

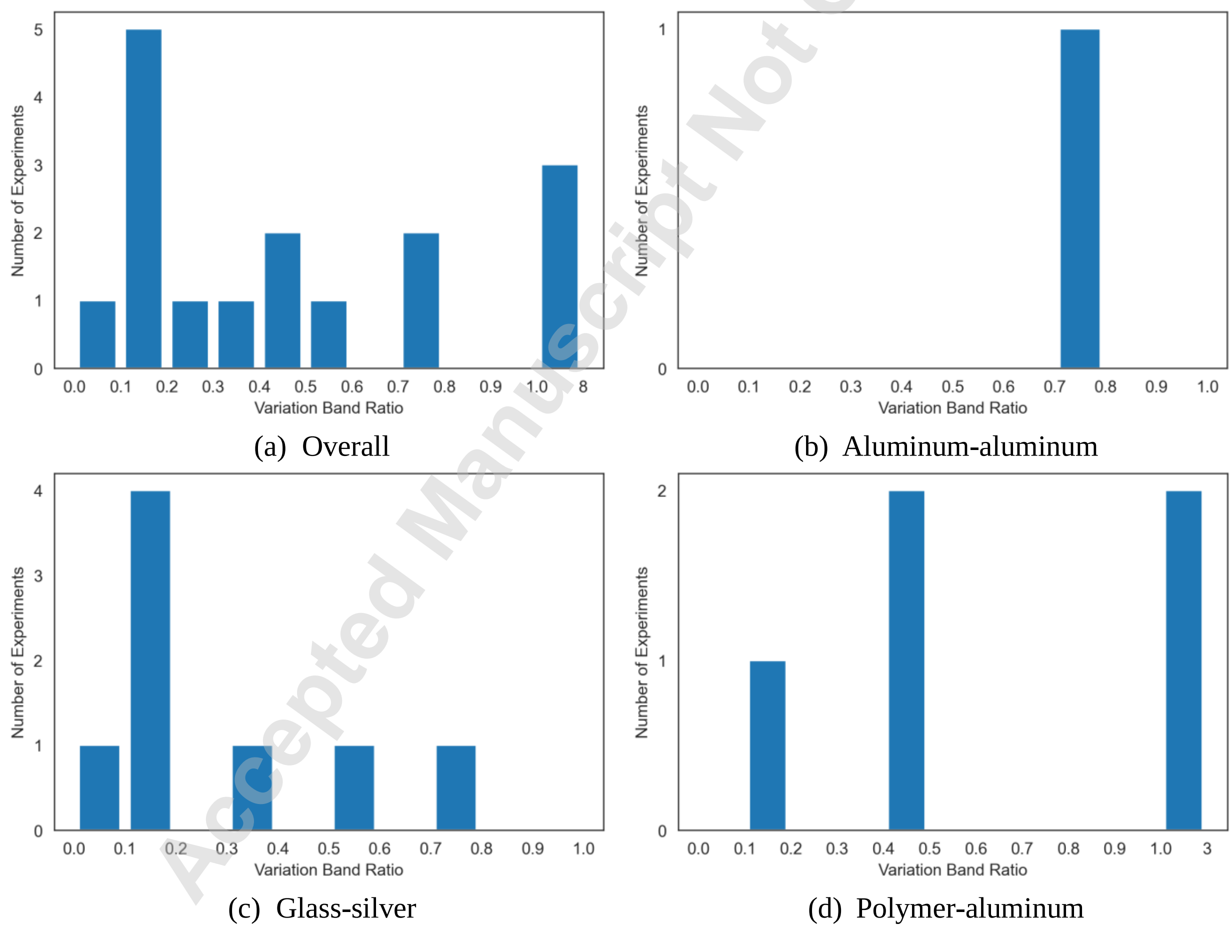

(a) Overall

(b) Aluminum-aluminum

(c) Glass-silver

(d) Polymer-aluminum

Journal of Solar Energy Engineering. Received October 14, 2022;
Accepted manuscript posted June 22, 2023. doi:10.1115/1.4063079

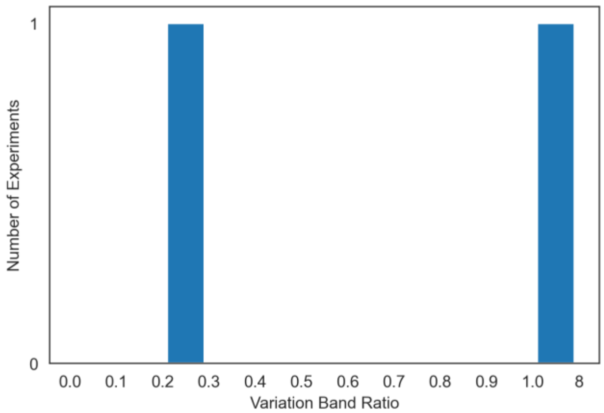

(e) Polymer-silver

Figure 6: Variation-band ratio statistics with respect to materials of mirrors. X axis is the interval that the ratio value belongs to. The Y axis is the number of mirrors counted in the corresponding interval.

4.4.4 Comparison of wavelength-dependent results

Based on the acceleration factors averaged over the 250–2,500 nm spectrum in Table 10, we compare the measured reflectance from XALE against all applicable outdoor conditions to see if the acceleration factor matches our measurement results. For an average acceleration factor, AF, of a given experiment, we iterate through each set of XALE measurements at the exposure duration t. We then implement a tolerance coefficient, k, and bound the outdoor durations that fall within the resulting bounds. If a perfect correlation occurs at k = 0, the upper bound b_u , in exposure months, is given by:

$$b_u = tAF(1.0 + k) \tag{4}$$

And the lower bound b_l, in exposure months, is given by:

$$b_l = tAF(1.0 - k) \tag{5}$$

The reported difference of the mean value is then

$$\delta = AF - AF_{ac} \tag{6}$$

Where AF is the average acceleration factor reported in Table 10, and AF_{ac} is the acceleration factor computed between the two identified conditions.

Using the DunMore-1 experiment listed in Table 11 as an example, the average AF = 3.8 from Table 10, between XALE and Golden, CO. There are two measurement sets available for the XALE condition: one at t_1=3.06 months and another at t_2=6.24 months. Using the formulation in Equations (4), (5) and (6) and a tolerance coefficient of k = 0.2, we bound the exposure durations for possible outdoor conditions for t_1 and t_2, which places the possible outdoor conditions corresponding with t_1 between 9.30 months and

Journal of Solar Energy Engineering. Received October 14, 2022;
Accepted manuscript posted June 22, 2023. doi:10.1115/1.4063079

13.95 months and the possible outdoor conditions corresponding with t_2 between 18.97 months and 28.45 months.

With the above bounds, we pair the available reflectance measurements for the Golden, CO outdoor condition at 13.56 months with condition 1, and the Golden, CO outdoor condition at 21.49 months with condition 2. The difference in the mean value is reported as the difference between the average acceleration factor AF and the computed acceleration factor from the given conditions. The results for the DunMore-1 example can be seen in Table 10 below.

In future acceleration testing, this enables scheduling measurements in accordance with the reported acceleration factors to further validate numerical results.

Table 10: Comparison between XALE and outdoor testing degradation rates in matched time.

Experiment	Test Condition	Exposure Month	XALE Time	Acceleration Factor	Difference of Mean Value	Material
3M_Northbridge-6	Golden, CO	45.37	5.15	9.18	11.22	Polymer-Silver
AirlightEnergy-1	Golden, CO	18.7	0.88	22.49	4.31	Polymer-Aluminum
Alanod-8	Golden, CO	3.15	6.76	0.44	1.34	Polymer-Aluminum
Alanod-8	Golden, CO	6.84	14.73	0.44	0.82	Polymer-Aluminum
Alanod-8	Golden, CO	6.84	17.61	0.44	0.86	Polymer-Aluminum
Alanod-8	Golden, CO	9.19	19.91	0.44	0.87	Polymer-Aluminum
Alanod-8	Miami, FL	12	17.61	0.66	0.62	Polymer-Aluminum
Alanod-8	Miami, FL	12	19.91	0.66	0.63	Polymer-Aluminum
Alanod-8	Phoenix, AZ	6.08	17.61	0.34	0.64	Polymer-Aluminum
Alanod-8	Phoenix, AZ	6.08	19.91	0.34	0.67	Polymer-Aluminum
Alcoa-11	Golden, CO	9.2	4.13	2.36	1.30	Polymer-Aluminum
Alcoa-11	Golden, CO	12.76	6.65	2.36	0.97	Polymer-Aluminum
Alcoa-11	Golden, CO	19.28	9.11	2.36	1.79	Polymer-Aluminum
Alcoa-11	Miami, FL	11.84	16.73	0.69	0.91	Polymer-Aluminum
Alcoa-11	Miami, FL	11.84	19.03	0.69	0.92	Polymer-Aluminum
Alcoa-11	Phoenix, AZ	12	13.85	0.99	0.76	Polymer-Aluminum
Alcoa-12	Golden, CO	8.25	4.13	2.12	0.75	Polymer-Aluminum
Alcoa-12	Golden, CO	11.81	6.65	2.12	0.77	Polymer-Aluminum

Journal of Solar Energy Engineering. Received October 14, 2022;
Accepted manuscript posted June 22, 2023. doi:10.1115/1.4063079

Alcoa-12	Golden, CO	18.33	9.11	2.12	1.55	Polymer-Aluminum
Alcoa-12	Golden, CO	24.48	13.85	2.12	0.57	Polymer-Aluminum
DunMore-1	Golden, CO	13.56	3.06	3.80	1.38	Aluminum-Aluminum
DunMore-1	Golden, CO	21.49	6.24	3.80	1.63	Aluminum-Aluminum
Fenzi-1	Golden, CO	4.68	5.58	0.98	2.86	Glass-Silver
Fenzi-1	Golden, CO	13.66	13.85	0.98	3.42	Glass-Silver
Fenzi-1	Golden, CO	16.75	16.39	0.98	0.52	Glass-Silver
Flabeg-3	Golden, CO	14.64	5.22	3.18	1.08	Glass-Silver
Flabeg-3	Golden, CO	28.13	8.31	3.18	1.60	Glass-Silver
Flabeg-3	Phoenix, AZ	22.1	12.74	1.52	0.91	Glass-Silver
Flabeg-3	Phoenix, AZ	22.1	16.53	1.52	0.20	Glass-Silver
JDSU-1	Phoenix, AZ	12	5.24	2.58	1.56	Glass-Aluminum
JDSU-1	Phoenix, AZ	24	7.86	2.58	0.68	Glass-Aluminum
Naugatuck-17	Golden, CO	11.67	1.64	8.24	0.67	Glass-Silver
Naugatuck-17	Golden, CO	37.62	5.47	8.24	0.93	Glass-Silver
Naugatuck-9	Golden, CO	20.1	5.77	3.96	5.22	Glass-Silver
Naugatuck-9	Golden, CO	66.17	20.39	3.96	0.61	Glass-Silver
SaintGobain-1a	Phoenix, AZ	10.1	8.67	1.34	1.50	Glass-Silver
SaintGobain-1a	Phoenix, AZ	22.1	15.99	1.34	1.77	Glass-Silver
SaintGobain-1a	Phoenix, AZ	22.1	18.26	1.34	1.22	Glass-Silver
Samsung-2	Phoenix, AZ	22.1	5.47	3.62	2.62	Glass-Silver
SolarSystems-20	Golden, CO	35.56	1.05	34.94	3.39	Glass-Silver
SolarSystems-23	Golden, CO	10.39	1.19	8.99	0.18	Glass-Silver
SolarSystems-23	Golden, CO	14.08	1.95	8.99	0.53	Glass-Silver

Journal of Solar Energy Engineering. Received October 14, 2022;
Accepted manuscript posted June 22, 2023. doi:10.1115/1.4063079

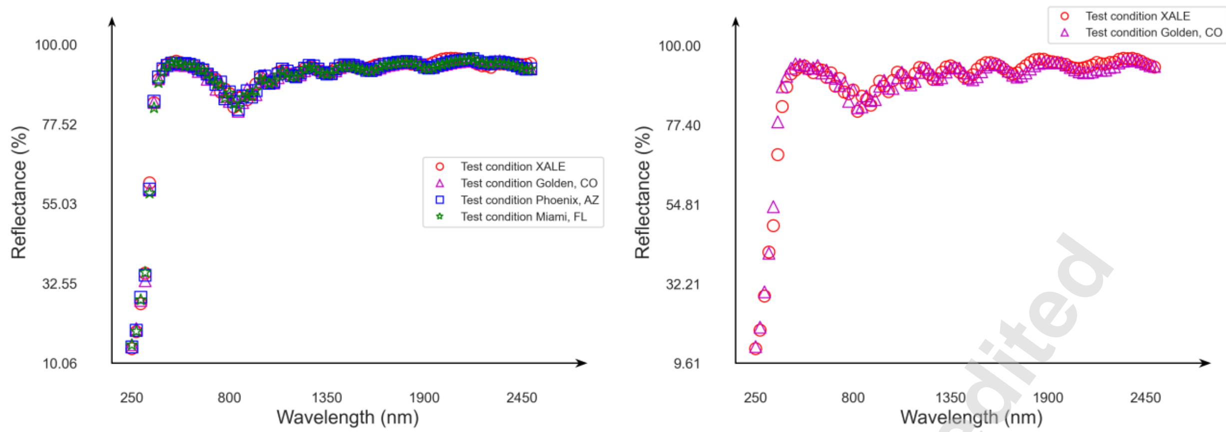

(a) Alanod-8 at Golden, CO with exposure month = 6.84; Miami, FL with exposure month = 12; Phoenix, AZ with exposure

(b) Alanod-11 at Golden, CO with exposure month = 9.2; at XALE with exposure month = 4.13.

Figure 7: Full spectral reflectance for two Alanod front-surface aluminum samples, showing strong agreement between the computed acceleration factor in Table 10 and the outdoor results.

Figure 7 above shows results for two Alanod mirror samples weathered in two test conditions. Shown in Figure 7 (a), we see the applied XALE condition requires longer exposure to match outdoor test conditions. In Figure 7 (b) we see a strong correlation between roughly 4 months in an accelerated condition when compared with 9 months outdoors. These results suggest longer-term exposures are needed for accurate modeling. Long-term outdoor exposure experimental data is one of the main benefits of the SMMD.

4.4.5 Statistical analyses on wavelength-dependent results

Comparison of the outdoor and XALE test chamber reflectance distributions require two statistical tests to determine equivalence. A two-sample t-test tests the equality of values at each wavelength, and a two-sample KS statistic tests the equality of shapes. Each test is described below, and following each description representative distributions are provided, tested, and results explained. The summary of results is provided in Table 11.

The first test, a two-sample t-test, compares the distribution of the reflectance differences between the outdoor test and XALE test for each sample. If the reflectance values between outdoor and XALE are the same, the distribution of differences should have a mean near 0, consistent with measurement uncertainty. This is the null hypothesis. Measurement uncertainty is a function of many parameters but is here estimated as having a standard deviation of 0.34% based on convolving surface non-uniformity results (see Table 12, $\frac{1.59}{\sqrt{25}} = 0.32$) and instrument repeatability. The p-value associated with the two-sample t-test is the probability of the outdoor data having the same or larger distribution of differences assuming that the null hypothesis is true: i.e., the differences are zero-mean. A p-value less than or equal to 0.05 indicates that the differences are NOT zero-mean, and therefore the outdoor and XALE tests are not the same and acceleration factors between the two should not be computed. If the p-value is greater than 0.05, then the differences are consistent with zero mean (the "same") at a significance level of 95%.

For example, consider the comparison of the Golden, CO and XALE samples in the 3M-Northbridge-6 experiment, as shown below.

Journal of Solar Energy Engineering. Received October 14, 2022;
Accepted manuscript posted June 22, 2023. doi:10.1115/1.4063079

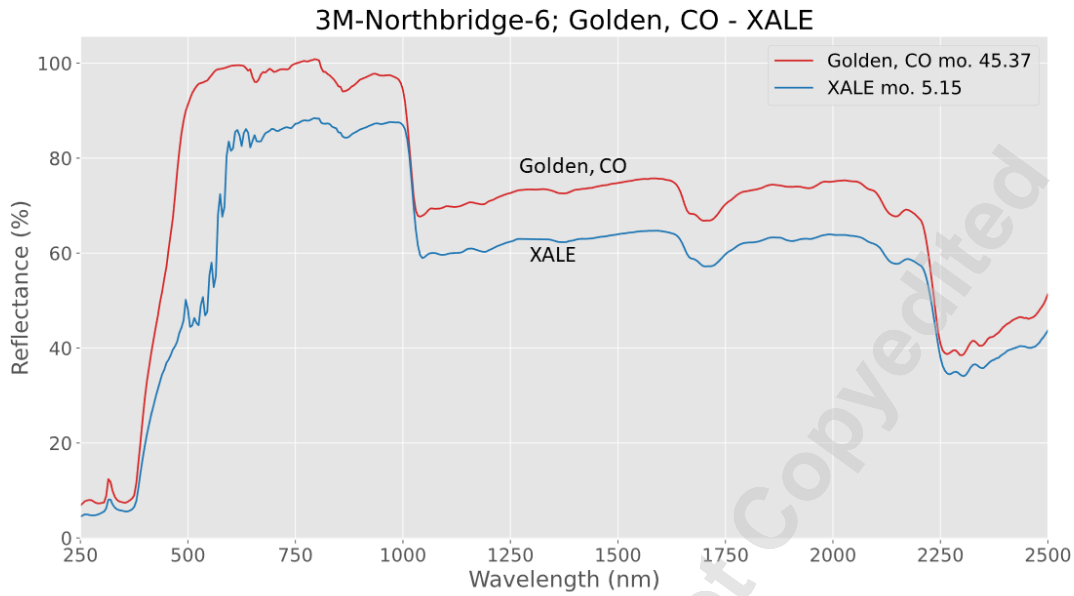

Figure 8: Spectral comparison of 3M Northbridge mirror exposed outdoors in Golden, CO (upper trace) for 45 months and indoors using a XALE weatherometer (lower trace) at 5 months.

The Golden, CO outdoor sample was measured at 45.37 months, the XALE sample at 5.15 months. Ideally, the distributions would have the same values at each wavelength, thereby ensuring that the overall solar-weighted reflectance would be the same. However, as can be seen in the plot above, at many wavelengths there are large differences (on the order of 10%) between the Golden and XALE distributions. Calculating these differences at each wavelength and plotting their distribution results in Figure 9:

Journal of Solar Energy Engineering. Received October 14, 2022;
Accepted manuscript posted June 22, 2023. doi:10.1115/1.4063079

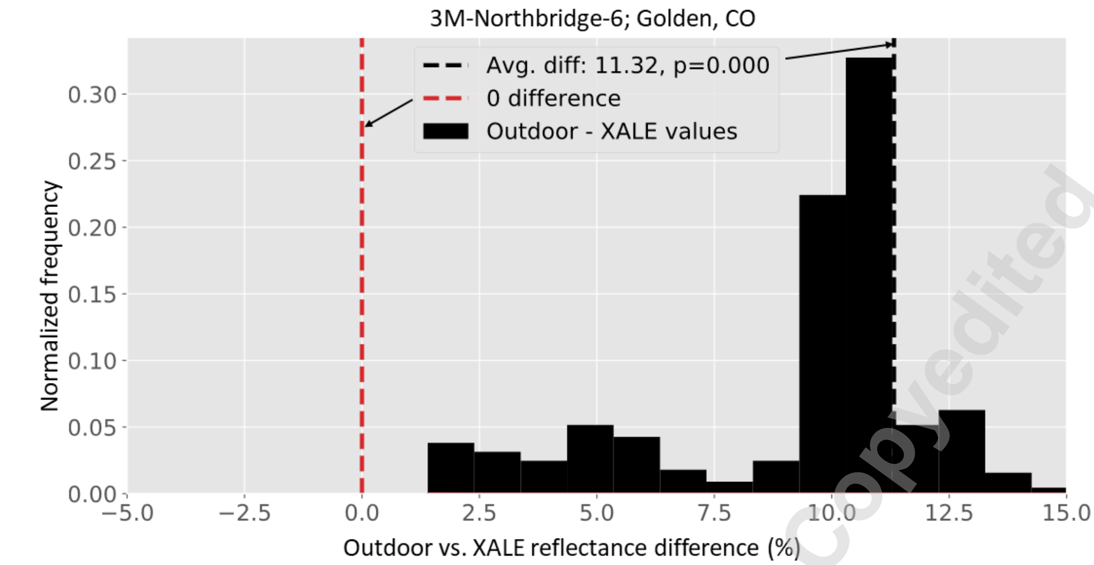

Figure 9: Histogram showing frequency of wavelength-dependent differences in reflectance with an average difference of 11.32% across the applied spectrum.

The average difference between the Golden, CO and XALE distributions is 11.32%, which along with the p-value suggests the computation of an acceleration factor from these distributions is inappropriate.

Contrast this with the Golden, CO and XALE samples of the Alanod-8 experiment at 9 and 19 months in Figure 10.

Journal of Solar Energy Engineering. Received October 14, 2022;
Accepted manuscript posted June 22, 2023. doi:10.1115/1.4063079

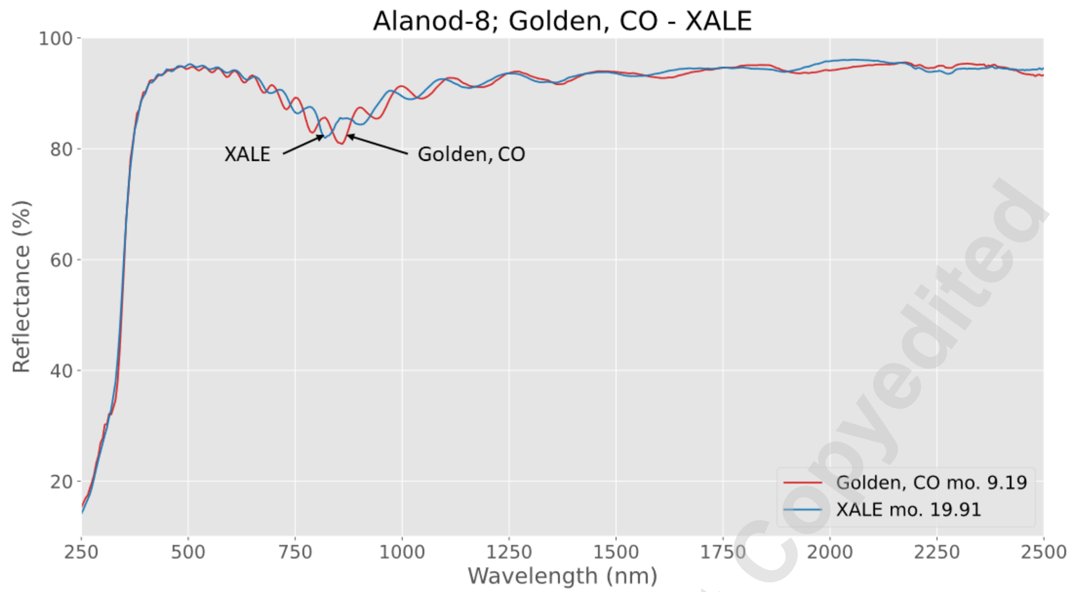

Figure 10: Spectral comparison of Alanod-8 mirror exposed outdoors in Golden, CO for 9 months and indoors using a XALE weatherometer at 19 months.

Here, the distributions align more closely at each wavelength. The histogram in Figure 11 shows the wavelength-dependent differences are near 0 with a p-value of 0.58, suggesting this pairing is more appropriate for calculating an acceleration factor.

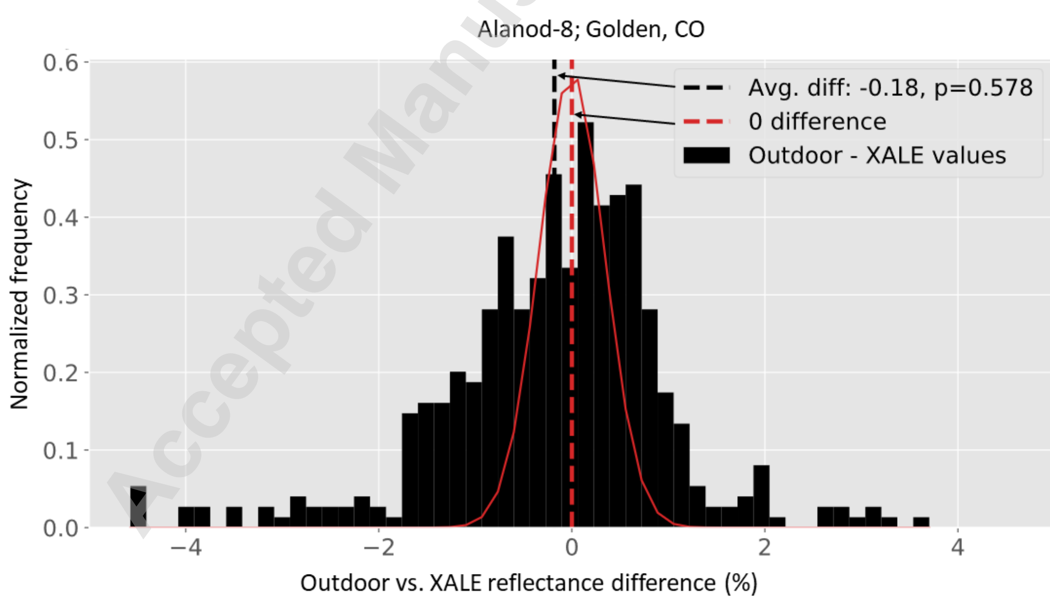

Figure 11: Distribution of difference in reflection for Alanod-8 mirror exposed in Golden, CO for 9 months and indoors use a XALE weatherometer at 19 months.

Journal of Solar Energy Engineering. Received October 14, 2022;
Accepted manuscript posted June 22, 2023. doi:10.1115/1.4063079

The second test, a two-sample Kolmogorov-Smirnov (KS) test, quantifies through comparison of cumulative distributions whether the shapes of two distributions are the same. If the distributions have the same shape, then the maximum vertical difference between their cumulative distributions for this data should be zero. This would indicate that the shapes (not the absolute values) of the distributions are similar: they have degraded qualitatively in the same way. For the number of datapoints in each of the distributions, a KS critical value of 0.09 or less determines to 95% confidence if the shape of the distributions can be considered the same.

For example, consider the distributions of the Samsung-2 experiment between samples weathered outdoor in Phoenix, AZ at 22.1 months and XALE at 5.47 months shown in Figure 12.

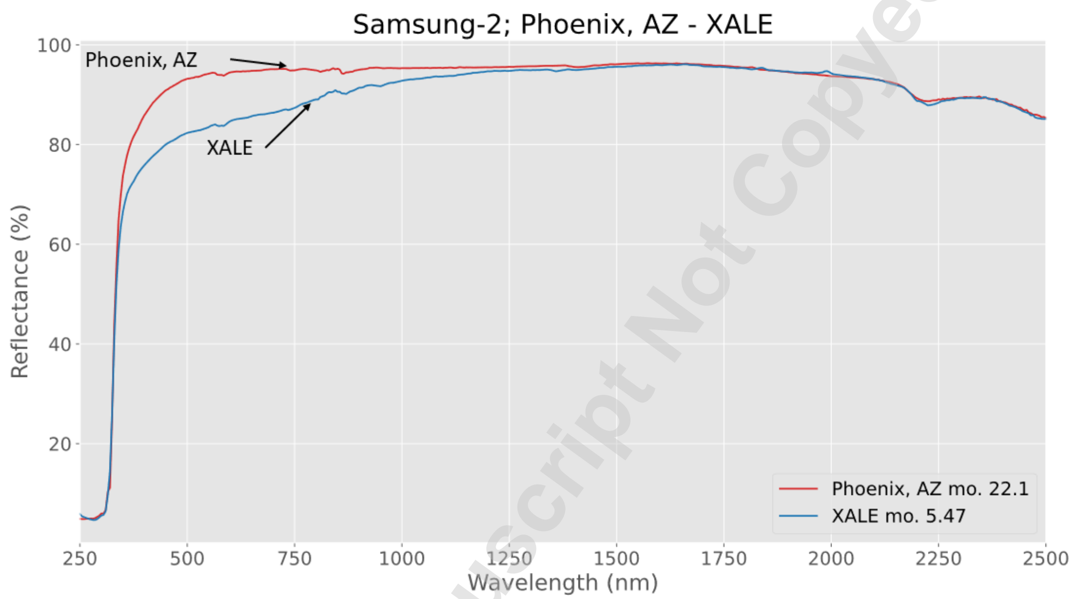

Figure 12: Spectral comparison of a Samsung mirror exposed outdoors in Phoenix, AZ for 22 months and indoors using a XALE weatherometer at 5.5 months.

There are reflectance differences between the two less at wavelengths less than 1,250 nm, but beyond that their shape is roughly the same. Figure 13 below finds the maximum vertical difference between the cumulative distribution functions of each distribution.

Journal of Solar Energy Engineering. Received October 14, 2022;
Accepted manuscript posted June 22, 2023. doi:10.1115/1.4063079

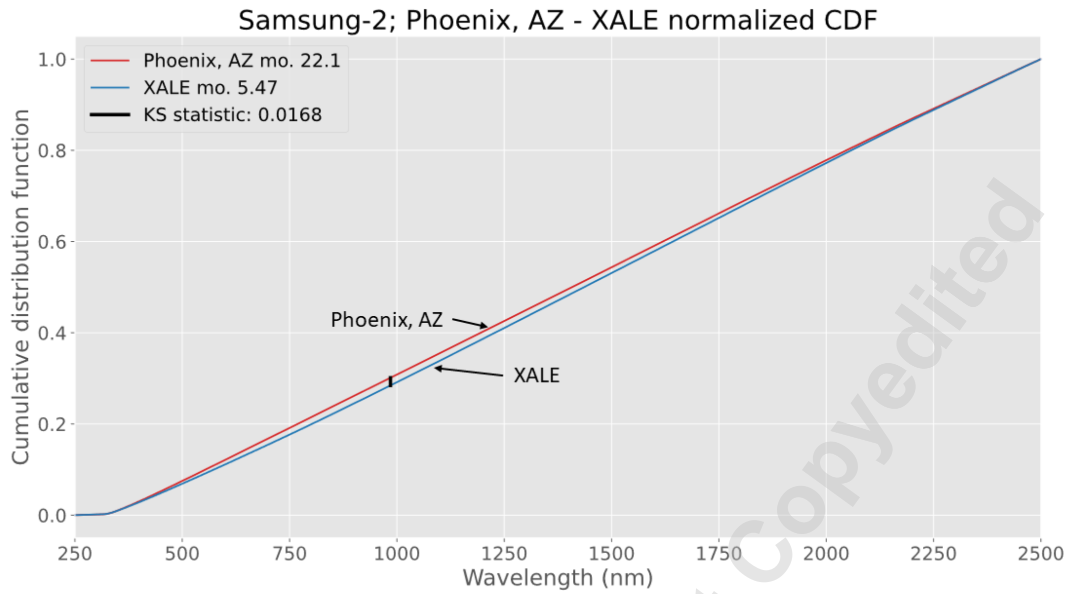

Figure 13: Normalized cumulative distribution function (CDF) showing the cumulative differences in reflectance per wavelength resulting in a KS statistic of 0.0168.

The maximum vertical difference between the cumulative distribution functions – 0.0168 – occurs just under 1,000 nm. This difference is less than 0.09, so to 95% confidence the two distributions can be said to have the same shape.

Table 11 below summarizes the acceleration factor, the mean difference, and the results of the t-tests and KS-tests for the indicated experiment sample pairings. Reflectance was compared prior to exposure to ensure appropriate comparisons were made between XALE and outdoor conditions.

Table 11: Statistical test results for all experimental sample pairings.

Experiment	Test condition	Exposure month	XALE time	Acceleration factor	Mean diff. (%)	t-test p-value	t-test concl.	KS statistic	KS concl.	Material
3M_Northbridge -6	Golden, CO	45.37	5.15	9.18	11.3	0.000	Not same	0.031	Same	Polymer-Silver
AirlightEnergy-1	Golden, CO	18.7	0.88	22.49	3.3	0.000	Not same	0.005	Same	Polymer-Aluminum
Alanod-8	Golden, CO	3.15	6.76	0.44	-1.3	0.000	Not same	0.002	Same	Polymer-Aluminum
Alanod-8	Golden, CO	6.84	14.73	0.44	-0.4	0.220	Same	0.001	Same	Polymer-Aluminum
Alanod-8	Golden, CO	6.84	17.61	0.44	-0.1	0.681	Same	0.001	Same	Polymer-Aluminum
Alanod-8	Golden, CO	9.19	19.91	0.44	-0.2	0.578	Same	0.001	Same	Polymer-Aluminum
Alanod-8	Miami, FL	12	17.61	0.66	-0.4	0.183	Same	0.001	Same	Polymer-Aluminum
Alanod-8	Miami, FL	12	19.91	0.66	-0.3	0.292	Same	0.001	Same	Polymer-Aluminum
Alanod-8	Phoenix, AZ	6.08	17.61	0.34	-0.1	0.679	Same	0.001	Same	Polymer-Aluminum
Alanod-8	Phoenix, AZ	6.08	19.91	0.34	0.0	0.889	Same	0.001	Same	Polymer-Aluminum

Journal of Solar Energy Engineering. Received October 14, 2022;
Accepted manuscript posted June 22, 2023. doi:10.1115/1.4063079

Alcoa-11	Golden, CO	9.2	4.13	2.36	-0.1	0.807	Same	0.005	Same	Polymer-Aluminum
Alcoa-11	Golden, CO	12.76	6.65	2.36	0.2	0.631	Same	0.004	Same	Polymer-Aluminum
Alcoa-11	Golden, CO	19.28	9.11	2.36	-0.6	0.073	Same	0.004	Same	Polymer-Aluminum
Alcoa-11	Miami, FL	11.84	16.73	0.69	0.5	0.121	Same	0.001	Same	Polymer-Aluminum
Alcoa-11	Miami, FL	11.84	19.03	0.69	0.6	0.078	Same	0.001	Same	Polymer-Aluminum
Alcoa-11	Phoenix, AZ	12	13.85	0.99	0.5	0.100	Same	0.003	Same	Polymer-Aluminum
Alcoa-12	Golden, CO	8.25	4.13	2.12	0.0	0.952	Same	0.001	Same	Polymer-Aluminum
Alcoa-12	Golden, CO	11.81	6.65	2.12	0.3	0.375	Same	0.001	Same	Polymer-Aluminum
Alcoa-12	Golden, CO	18.33	9.11	2.12	-0.7	0.027	Not same	0.002	Same	Polymer-Aluminum
Alcoa-12	Golden, CO	24.48	13.85	2.12	-0.1	0.851	Same	0.002	Same	Polymer-Aluminum
DunMore-1	Golden, CO	13.56	3.06	3.80	-1.3	0.000	Not same	0.006	Same	Aluminum-Aluminum
DunMore-1	Golden, CO	21.49	6.24	3.80	-1.6	0.000	Not same	0.005	Same	Aluminum-Aluminum
Fenzi-1	Golden, CO	4.68	5.58	0.98	-2.5	0.000	Not same	0.006	Same	Glass-Silver
Fenzi-1	Golden, CO	13.66	13.85	0.98	-4.0	0.000	Not same	0.004	Same	Glass-Silver
Fenzi-1	Golden, CO	16.75	16.39	0.98	-0.6	0.069	Same	0.001	Same	Glass-Silver
Flabeg-3	Golden, CO	14.64	5.22	3.18	-1.2	0.000	Not same	0.001	Same	Glass-Silver
Flabeg-3	Golden, CO	28.13	8.31	3.18	-1.7	0.000	Not same	0.005	Same	Glass-Silver
Flabeg-3	Phoenix, AZ	22.1	12.74	1.52	-0.8	0.013	Not same	0.005	Same	Glass-Silver
Flabeg-3	Phoenix, AZ	22.1	16.53	1.52	0.1	0.655	Same	0.001	Same	Glass-Silver
JDSU-1	Phoenix, AZ	12	5.24	2.58	-0.7	0.049	Not same	0.005	Same	Glass-Aluminum
JDSU-1	Phoenix, AZ	24	7.86	2.58	-0.2	0.583	Same	0.002	Same	Glass-Aluminum
Naugatuck-17	Golden, CO	11.67	1.64	8.24	0.1	0.796	Same	0.004	Same	Glass-Silver
Naugatuck-17	Golden, CO	37.62	5.47	8.24	-0.9	0.007	Not same	0.003	Same	Glass-Silver
Naugatuck-9	Golden, CO	20.1	5.77	3.96	0.5	0.453	Same	0.022	Same	Glass-Silver
Naugatuck-9	Golden, CO	66.17	20.39	3.96	-0.3	0.401	Same	0.002	Same	Glass-Silver
SaintGobain-1a	Phoenix, AZ	10.1	8.67	1.34	-1.4	0.000	Not same	0.003	Same	Glass-Silver
SaintGobain-1a	Phoenix, AZ	22.1	15.99	1.34	-1.7	0.000	Not same	0.001	Same	Glass-Silver
SaintGobain-1a	Phoenix, AZ	22.1	18.26	1.34	-1.1	0.001	Not same	0.002	Same	Glass-Silver
Samsung-2	Phoenix, AZ	22.1	5.47	3.62	2.6	0.000	Not same	0.017	Same	Glass-Silver
SolarSystems-20	Golden, CO	35.56	1.05	34.94	-3.4	0.000	Not same	0.007	Same	Glass-Silver
SolarSystems-23	Golden, CO	10.39	1.19	8.99	0.0	0.887	Same	0.001	Same	Glass-Silver
SolarSystems-23	Golden, CO	14.08	1.95	8.99	0.0	0.904	Same	0.003	Same	Glass-Silver

Journal of Solar Energy Engineering. Received October 14, 2022;
Accepted manuscript posted June 22, 2023. doi:10.1115/1.4063079

5 Discussion & Conclusions

The analysis above extracts experiments and analyzes trends in degradation from NREL's SMMD. The database contains over 100,000 measurements taken since NREL began cataloguing reflectance data in 1980. The data shown suggest that in many cases, a linear fit for degradation can be appropriate, yielding encouraging correlation statistics. Modeling the degradation in this manner can be used to validate accelerated indoor weathering tests. NREL's current standard XALE test utilizes 60°C, 60% RH, and two suns DNI. The data analyzed herein can be used to provide evidence to the efficacy of that condition, allowing test designs to be modified appropriately to mimic outdoor conditions at an accelerated rate.

For example, in the condition shown in Figure 8, a strong outdoor correlation trend is identified, as is a strong indoor correlation. The KS test result suggests the sample is degrading in a similar manner. Going forward, the test may be designed with the same environmental stressors but modifying exposure time to achieve a stronger acceleration factor. In the case of the Naugatuck-17 mirror shown in Table 10 and Table 11, we see strong correlation in the outdoor condition and a strong correlation in the indoor condition independently, but the statistical analysis suggests the degradation modes are not equivalent. To purposefully recreate this experiment, closer attention should be paid to the environmental stress inputs.

This paper is not meant to claim the analysis herein is the only or most beneficial analysis to be conducted. The compilation of this volume of data, now accessible to the solar mirror and CSP community, provides a tremendous resource for comparing models and accelerated degradation experiments against naturally degraded samples with decades-long durability. This analysis is to act as a foundation that may assist in experiment design when modeling accelerated solar mirror degradation. The analysis, in many cases, shows that degradation of solar mirrors can be largely attributed to the climate-specific conditions they're designed to operate in: elevated temperatures, varying levels of humidity, and constant solar irradiation.

NREL's SMMD is a tremendous resource for solar mirror aging data dating back to 1980. It contains information from various mirror types, manufacturers, and years. The data presented herein is an in-depth investigation into degradation trends among the data collected over the past 40 years. Identifying the trends and dependencies for solar mirror degradation is an integral step into accurately modeling solar mirror life cycles and developing accurate and reliable accelerated aging procedures. These accelerated aging methods are crucial to guiding the design and manufacture of effective and durable solar mirrors.

6 Future Work

The data presented in this paper presents a foundation from which to base future degradation experiments. Mirror degradation experiments and procedures have largely been adapted from other industries, which may not necessarily subject the mirrors to their most relevant environmental stressors. The investigation here offers a large body of data in both accelerated conditions, and the more difficult to procure, naturally occurring degradation conditions that a solar mirror will see over its lifetime. From it, we can see impacts to reflectance due to temperature, irradiance, and humidity in a variety of climates. An analysis in both overall solar-weighted value and wavelength-dependent reflectance losses may help to design experiments in the future based on mirror type, climate, or receiver properties.

Understanding fundamental mechanisms for solar mirror degradation is integral to designing useful methods and guidelines for accelerated aging tests. There is work to be done to further our understanding of the processes governing degradation. More complex fitting analyses can be done on existing data, machine learning can be implemented once the database grows to a suitable volume to train useful

Journal of Solar Energy Engineering. Received October 14, 2022;
Accepted manuscript posted June 22, 2023. doi:10.1115/1.4063079

models, and the state-of-the-art is constantly progressing. This requires on ongoing body of research to adequately keep pace and understand how these new mirrors will behave throughout their life cycle.

In addition, the primary metrics used in this database analysis are the hemispherical and specular reflectance. These are the most influential parameters governing energy losses at the mirror surface. These metrics, however, are resultant of the condition of the mirror itself. Degradation results in reflectance losses, but the underlying cause may be pitting, corrosion, microfracture, delamination, or a combination of chemical and physical changes to the reflector. Characterizing and linking these degradation mechanisms to levels of environmental stress could yield high accuracy life cycle models based on not only the reflector itself, but the environment for which it was designed. The optimal mirror for a dry climate with coarse sand may differ substantially from the optimal mirror from a coastal climate with high humidity and airborne salts, for example. Table 12 below highlights some material characterization techniques that may be useful in future experiments.

Table 12: Material properties characterization technologies.

Property Evaluated	Method Required	Availability
Lattice Parameter/Composition	X-ray diffraction	National Renewable Energy Laboratory (NREL), Commissariat à l'énergie atomique et aux énergies alternatives (CEA)
Transmittance/Reflectance	UV-vis spectrometer, variable-angle spectroscopic ellipsometry, Rutherford backscattering	NREL, CEA, Centro de Investigaciones Energéticas, Medioambientales y Tecnológicas (CIEMAT), Deutsches Zentrum für Luft- und Raumfahrt (DLR)
Paint Layer Composition	FTIR, ATR (polymer material and pain characterization), FTIR handheld	NREL, CEA, DLR, CIEMAT
Diffusivity	Mocon, LFA (laser flash analysis)	NREL, CEA
Surface Roughness	AFM, profilometry	NREL, CEA, CIEMAT, DLR
Composition	Energy dispersion X-ray (EDX) and scanning electron microscopy (SEM)	CEA, CIEMAT, DLR
Composition	TEM (transmission electron microscopy: measuring corrosion of thin layer; e.g., Ag)	NREL, DLR (Cologne)
Contact Angle of Coatings	Contact angle	CEA, CIEMAT, DLR
Color/Gloss of Paints	Colorimeter	CEA

Acknowledgement

This work was authored in part by the National Renewable Energy Laboratory, operated by Alliance for Sustainable Energy, LLC, for the U.S. Department of Energy (DOE) under Contract No. DE-AC36-08GO28308. Funding provided by U.S. Department of Energy Office of Energy Efficiency and Renewable Energy Solar Energy Technologies Office. The views expressed in the article do not necessarily represent the views of the DOE or the U.S. Government. The U.S. Government retains and the

publisher, by accepting the article for publication, acknowledges that the U.S. Government retains a nonexclusive, paid-up, irrevocable, worldwide license to publish or reproduce the published form of this work, or allow others to do so, for U.S. Government purposes.

References

[1] Avenel, C., Raccurt, O., Gardette, J.-L., and Therias, S., 2018, "Review of Accelerated Ageing Test Modelling and Its Application to Solar Mirrors," Solar Energy Materials and Solar Cells, **186**, pp. 29–41. https://doi.org/10.1016/j.solmat.2018.06.024

[2] Soni, V. K., Shrivastava, R. L., Untawale, S. P., and Shrivastava, K., 2018, "Performance Analysis and Optimization of Fresnel Lens Concentrated Solar Water Heater," Journal of Solar Energy Engineering, **141**(031010). https://doi.org/10.1115/1.4041846

[3] Girard, R., Delord, C., Disdier, A., and Raccurt, O., 2015, "Critical Constraints Responsible to Solar Glass Mirror Degradation," Energy Procedia, **69**, pp. 1519–1528. https://doi.org/10.1016/j.egypro.2015.03.103

[4] Kennedy, C. E., and Terwilliger, K., 2005, "Optical Durability of Candidate Solar Reflectors," Journal of Solar Energy Engineering, **127**(2), pp. 262–269. https://doi.org/10.1115/1.1861926

[5] Zheng, B., Wong, L. P., Wu, L. Y. L., and Chen, Z., 2017, "Identifying Key Factors towards Highly Reflective Silver Coatings," Advances in Materials Science and Engineering, **2017**, pp. 1–12. https://doi.org/10.1155/2017/7686983

[6] Mehos, M., Turchi, C., Jorgenson, J., Denholm, P., Ho, C., and Armijo, K., 2016, *On the Path to SunShot - Advancing Concentrating Solar Power Technology, Performance, and Dispatchability*, NREL/TP-5500-65688 SAND-2016-2237 R, EERE Publication and Product Library, Washington, D.C. (United States).

[7] Sutter, F., Fernández-García, A., Wette, J., and Wiesinger, F., 2017, "6 - Assessment of Durability and Accelerated Aging Methodology of Solar Reflectors," *The Performance of Concentrated Solar Power (CSP) Systems*, P. Heller, ed., Woodhead Publishing, pp. 169–201.

[8] Zhu, G., Kearney, D., and Mehos, M., 2014, "On Characterization and Measurement of Average Solar Field Mirror Reflectance in Utility-Scale Concentrating Solar Power Plants," Solar Energy, **99**, pp. 185–202. https://doi.org/10.1016/j.solener.2013.11.009

[9] Guiheneuf, V., Riou, O., Delaleux, F., Logerais, P.-O., and Durastanti, J.-F., 2017, "Correlation Between Transmittance and LWIR Apparent Emissivity of Soda-Lime Glass During Accelerated Aging Test for Solar Applications," Journal of Solar Energy Engineering, **139**(041006). https://doi.org/10.1115/1.4036415

[10] Delord, C., Blaise, A., Fernandez-García, A., Martínez-Arcos, L., Sutter, F., and Reche-Navarro, T. J., 2016, "Soiling and Degradation Analysis of Solar Mirrors," AIP Conference Proceedings, **1734**(1), p. 090001. https://doi.org/10.1063/1.4949186

[11] DiGrazia, M., Gee, R., and Jorgensen, G., 2010, "ReflecTech® Mirror Film Attributes and Durability for CSP Applications," American Society of Mechanical Engineers Digital Collection, pp. 677–682. https://doi.org/10.1115/ES2009-90336

[12] Edfouf, Z., Guerguer, M., and Raccurt, O., 2015, "Glass and Polymeric Mirrors Ageing under Different Moroccan Weathers, an Application for CSP Power Plants," Energy Procedia, **69**, pp. 1508–1518.

Journal of Solar Energy Engineering. Received October 14, 2022;
Accepted manuscript posted June 22, 2023. doi:10.1115/1.4063079

https://doi.org/10.1016/j.egypro.2015.03.101

[13] Fernández-García, A., Martínez-Arcos, L., Sutter, F., Wette, J., Sallaberry, F., Erice, R., Diamantino, T., Carvalho, M. J., Raccurt, O., Pescheux, A.-C., Imbuluzqueta, G., and Machado, M., 2018, "Accelerated Aging Test of Solar Reflectors According to the New AENOR Standard – Results of a Round Robin Test," SolarPACES International Conference on Concentrating Solar Power and Chemical Energy Systems, September 26-29, 2017, Santiago, Chile, AIP Conference Proceedings, **2033**(1), p. 230003. https://doi.org/10.1063/1.5067231

[14] Grosjean, A., Le Baron, E., Pescheux, A.-C., and Disdier, A., 2021, "Accelerated Aging Tests and Characterizations of Solar Mirrors: Comparison of Combinations of Stress Factors on Degradation," Solar Energy Materials and Solar Cells, **220**, p. 110851. https://doi.org/10.1016/j.solmat.2020.110851

[15] Raccurt, O., Delord, C., Bouquet, C., and Couturier, R., 2014, "Correlation between Solar Mirror Degradation and Colorimetric Measurement of Protective Back Layer," Energy Procedia, **49**, pp. 1700–1707. https://doi.org/10.1016/j.egypro.2014.03.179

[16] Bouaddi, S., Ahmed, I., and mensour, O. A., 2016, "Modeling and Prediction of Reflectance Loss in CSP Plants Using a Non Linear Autoregressive Model with Exogenous Inputs (NARX)," *2016 International Renewable and Sustainable Energy Conference (IRSEC)*, November 14-17, 2016, Marrakech, Morocco, pp. 706–709. https://doi.org/10.1109/IRSEC.2016.7984071

[17] Wette, J., Sutter, F., Fernández-García, A., Lahlou, R., and Armstrong, P., 2018, "Standardizing Accelerated Aging Testing Conditions for Silvered-Glass Reflectors," SolarPACES International Conference on Concentrating Solar Power and Chemical Energy Systems, September 26-29, 2017, Santiago, Chile, AIP Conference Proceedings, **2033**(1), p. 230014. https://doi.org/10.1063/1.5067242

[18] Celvi, D., Schreiber, C., Tirawat, R., and Zhu, G., 2020, "Update on NREL Outdoor Exposure Campaign of Solar Mirrors," *ASME 2020 14th International Conference on Energy Sustainability*, American Society of Mechanical Engineers, June 17-18, 2020 Virtual, Online, p. V001T02A006. https://doi.org/10.1115/ES2020-1647

[19] "Standard Tables for Reference Solar Spectral Irradiances: Direct Normal and Hemispherical on 37° Tilted Surface" https://www.astm.org/g0173-03r20.html.

[20] Fernandez-Garcia, A., Sutter, F., Montecchi, M., Sallaberry, F., Heimsath, A., Heras, C., Le Baron, E., and Soum-Glaude, A., 2018, "SolarPACES Reflectance Guidelines V3." SolarPACES technical report, version 3.1, 2018, Tabernas, Spain.

[23] Mehos, M., Turchi, C., Vidal, J., Wagner, M., Ma, Z., Ho, C., Kolb, W., Andraka, C., and Kruizenga, A., 2017, *Concentrating Solar Power Gen3 Demonstration Roadmap*, NREL/TP-5500-67464, National Renewable Energy Lab. (NREL), Golden, CO (United States).

[24] Montecchi, M., 2013, "Approximated Method for Modelling Hemispherical Reflectance and Evaluating Near-Specular Reflectance of CSP Mirrors," Solar Energy, **92**, pp. 280–287. https://doi.org/10.1016/j.solener.2013.03.014

[25] Almanza, R., Hernández, P., Martínez, I., and Mazari, M., 2009, "Development and Mean Life of Aluminum First-Surface Mirrors for Solar Energy Applications," Solar Energy Materials and Solar Cells, **93**(9), pp. 1647–1651. https://doi.org/10.1016/j.solmat.2009.05.004

[26] Kempe, M. D., 2005, "Control of Moisture Ingress into Photovoltaic Modules," *Conference Record of the Thirty-First IEEE Photovoltaic Specialists Conference.*, January 3-7, 2005, Lake Buena Vista, FL, pp. 503–506. https://doi.org/10.1109/PVSC.2005.1488180